International Journal of Microwave and Wireless Technologies, 2009, 1(6), 461–468.
doi:10.1017/S1759078709990560

Multi-access antenna for an opportunistic radio mobile communication of fourth generation

WALID EL HAJJ, FRANÇOIS GALLÉE AND CHRISTIAN PERSON

A new model of two-access reconfigurable antennas for future mobile communication systems is presented in this article. This structure is based on a slot antenna with two separated access ports, isolated and matched at 1 and 2 GHz, respectively. The novelty of this element lies in the fact that first a filtering structure is integrated in the antenna, and then any additional switching or frequency path selecting components that would induce losses and noise degradation is suppressed. Such flexible structures are assumed to be used in a future opportunistic radio, incorporating special features of "spectrum sensing". The concept of the antenna illustrated by simulation and measurement is presented.

Keywords: Multi-access antenna, Opportunistic radio, Reconfigurable antenna, Spectrum sensing

Received 30 June 2009; Revised 8 September 2009; first published online 7 January 2010

I. INTRODUCTION

The future generation of mobile phones will certainly exploit the numerous advantages of opportunistic cognitive radio concepts. Indeed, a flexible system, aware of its immediate environment through sensing operating modes and dynamic reconfiguration properties, will offer greatest services and performances; it will therefore become possible to dynamically and autonomously adjust radio operating parameters depending on available and collaborating wireless and wired networks, then offering improved nomadism and ubiquitous performances. [1]

Access to such improved flexibility involves specific constraints on the RF and digital interfaces of mobile devices for optimizing the communication interfaces. In this context, the aim is to consider and to design the RF sub-system to be as simple as possible (especially concerning filtering stages and the selection part of operating standards) and to ensure analog/digital (A/D) and digital/analog (D/A) conversion operations as closely as possible to the antenna to enhance the digital reconfigurability of the system. The idea of this multi-access antenna is to enable the management of these multiple parallel access ports for both transmission/reception modes directly by software. The structure, in addition to simplifying the radio frequency (RF) part (improved isolation between adjacent frequency bands, selective ports, size, etc.), is suitable for multistandard operations and more generally for the implementation of the SDR (Software Defined Radio) in an opportunistic context.

In a multistandard context, classical radio architectures use two types of antenna structures:

- Multiband antennas with one access port (PIFA i.e. [2, 3], Patch i.e. [4], Meandered i.e. [5], etc.). In this case, RF filtering remains necessary, which induces limitations in terms of complexity, noise, performances and therefore, reliability with the SDR approach (Fig. 1(a)).
- Multi-access antennas, with channels selection using switches – i.e. [6] (Fig. 1(b)). This frequency band selection method induces constraints on the input impedance of the non-activated access ports (open circuit (OC) terminations usually for proper matching conditions), which is not quite always feasible in practice under wideband operating conditions.

Furthermore, this switching system limits the flexibility of the system dedicated to the SDR, including the operations of spectrum sensing (services availability survey) and real-time programming.

In this paper, the innovation of the proposed approach (Fig. 1(c)) consists in considering a two-access ports 50 Ω simultaneously matched antenna, with a quasi-omnidirectional radiation pattern, and then allowing direct-software standards selectivity and management without any switching or filtering operations. This approach is also compatible with radio front-end global integration on mature SiGe-type technologies.

II. ANTENNA DESIGN

A) Description of the structure

The antenna (see Fig. 2) is performed on a Rogers 4003 substrate ($\varepsilon_r = 3.38$) of dimensions $40.25 \times 95 \times 0.508$ mm^3. A slot is etched on the upper 40.25×43 mm^2 metallization level; two lumped feeding ports are inserted along one edge of this rectangular structure, each apart from the open-end extremities of the slot. Each of this access corresponds to a specific resonating mode, which can be selected independently from each other depending on the applied matching

Lab-STICC/MOM, Telecom Bretagne, Technopôle Brest-Iroise CS 83818, 29238 Brest Cedex 3, France.
Corresponding author:
W. El Hajj
Email: walid.elhajj@telecom-bretagne.eu

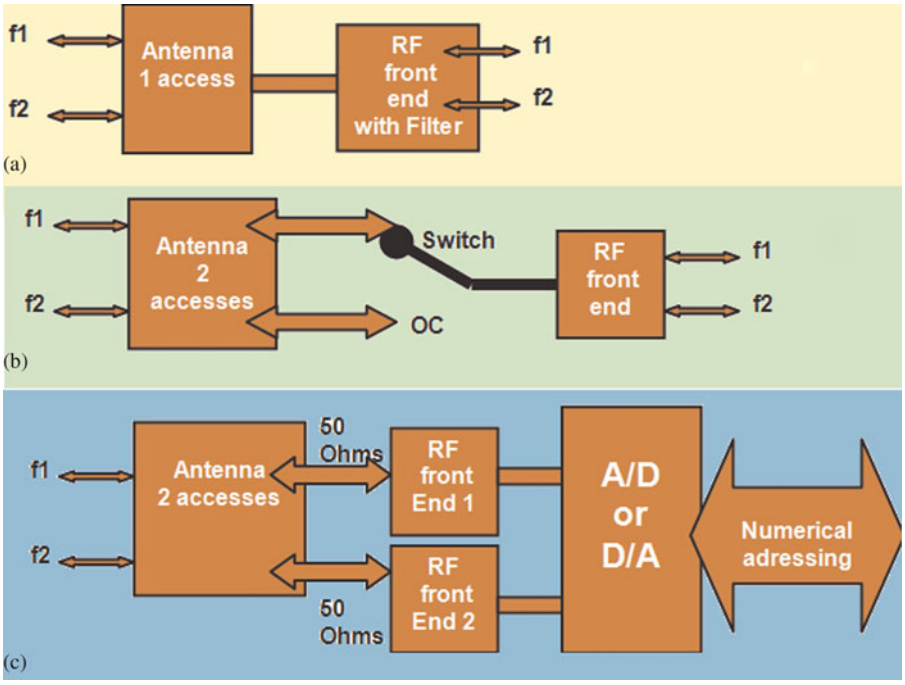

Fig. 1. Comparison between different architectures in a multistandard context. (a) Bi-band antenna with selective filtering input stage. (b) Bi-band antenna with selective switching structure. (c) Proposed architecture with two-access ports antenna and direct conversion (RF front ends without filter or switch).

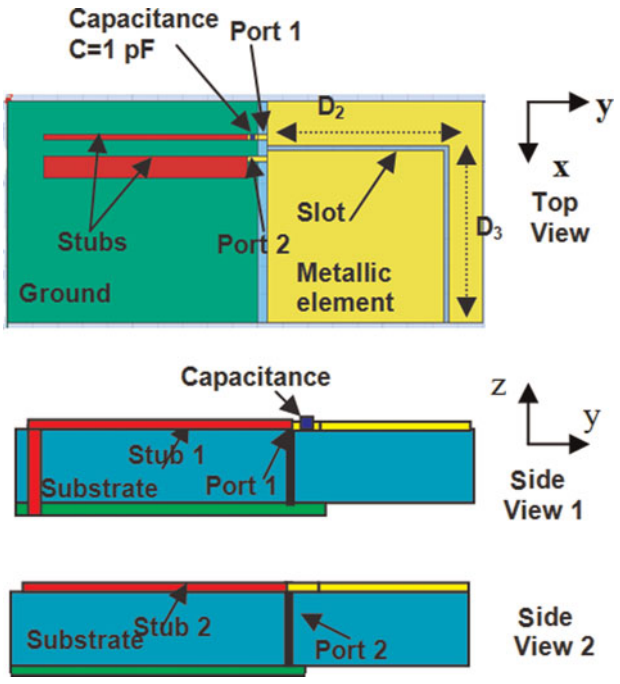

Fig. 2. Model of the antenna.

conditions. Consequently, we have a bi-access structure, with a potential bi-band behavior depending on the excitation structure.

Two microstrip stubs (in Fig. 2) are connected to the access ports 1 and 2; these stubs ensure the isolation of each of the operating modes towards the other [7]. A capacitance ($C = 1$ pF) is placed in series with port 1 to ensure the matching condition at its own operating frequency. A $40.25 \times 50\ \text{mm}^2$ ground plane is realized on the left side of the substrate lower level. The simulations were carried out using Ansoft/HFSS^{TM}, considering lumped port-type excitations. The results are presented in Fig. 4.

B) Analysis and operating principles

The objective is to design an antenna with two isolated ports, each operating at its own resonance frequency (f_1 for port 1 and f_2 for port 2). Such an achievement requires that the access port 1 (and respectively the access port 2) at frequency f_1 (and respectively at frequency f_2) is matched to 50 Ω, while the second access is loaded using an equivalent short circuit (SC) at f_1 (and respectively at f_2) (Fig. 3). The principle is explained in detail in Section II.C.

We can observe in Fig. 4 that for the operating mode 1 {port 1: excited, port 2: 50 Ω (port 2 is loaded by a 50 Ω impedance but we always have the condition that the equivalent impedance of port 2 at f_1 is an (SC) impedance as we explained before)}, the resonant frequency is $f_1 = 1.23$ GHz (relative

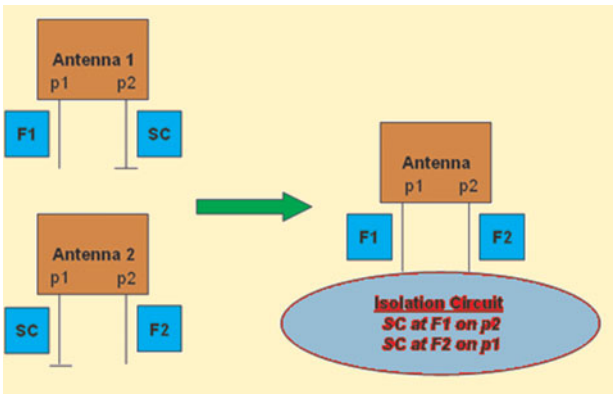

Fig. 3. Isolation principle of the two ports.

https://doi.org/10.1017/S1759078709990560 Published online by Cambridge University Press

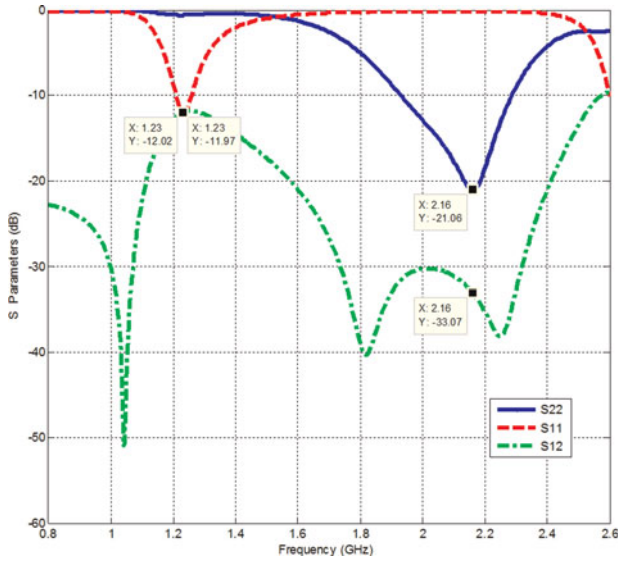

Fig. 4. Coupling and reflexion coefficients on the two accesses.

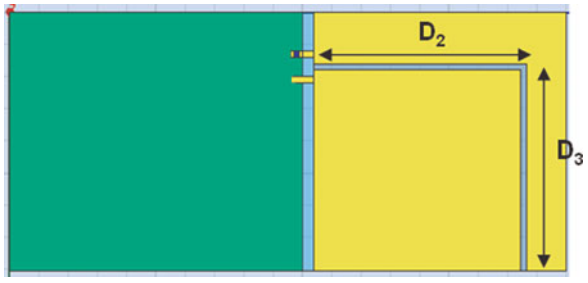

Fig. 5. Dimensions of the slot.

bandwidth #4% at $ROS = 2$). For mode 2 {port 2: excited, port 1: 50 Ω}, the resonant frequency is $f_2 = 2.16$ GHz (relative bandwidth #16% at $ROS = 2$). A 12 dB isolation value – see S_{21} parameter in Fig. 4 (30 dB respectively) between the access ports is obtained over the f_1 frequency band (and the f_2 frequency band, respectively), well above the 10 dB expected isolation threshold.

The dimensions D_2 and D_3 of the slot (Fig. 5) affect the frequency response of the antenna. We therefore proceed with a parametric simulation as a function of the slot lengths D_2 and D_3 for the antenna without the isolation circuit since it mainly contributes to the matching and isolation conditions, independently from the frequency resonances.

This parametric simulation was done according to antenna 1 (antenna 2, respectively) – see Fig. 3 – to study the influence of D_2 and D_3 on f_1 (and respectively on f_2). The results are reported in Fig. 6.

Referring to Fig. 6, the frequency f_1 is controlled by the distances D_2 and D_3, whereas f_2 is controlled by D_3 only. Figure 7 shows the current density distribution in the two excitation configurations. It confirms that f_1 is controlled by the distance $D_2 + D_3$, and f_2 is controlled by D_3, the maximum current density being distributed along the $D_2 + D_3$ path length for f_1 excitation conditions, and being concentrated along the D_3 path length for f_2 excitation conditions. This figure also shows that the radiating part of the structure is essentially related to the slot; the dimensions of the surrounding rectangular metallic parts (upper "patch" and the ground plane) influence the input impedance of the antenna (matching).

C) Open and SC stubs: incidence

We consider two operating frequencies (f_1 on port 1 – f_2 on port 2) so that $f_2 \approx 2f_1$. This choice is quite advantageous since both stubs have a dual behavior on ports 1 and 2 at f_1 and f_2, respectively.

A short circuited (SC) termination is chosen for the $\lambda g/2$ stub 1 (connected on port 1) at f_2 (and consequently $\lambda g/4$ at f_1). This length is selected so as to ensure SC conditions on port 1 at f_2, and OC conditions at f_1, simultaneously. Perfect matching and isolation situations can therefore be simultaneously obtained on the access port 1 at f_1 and f_2, respectively.

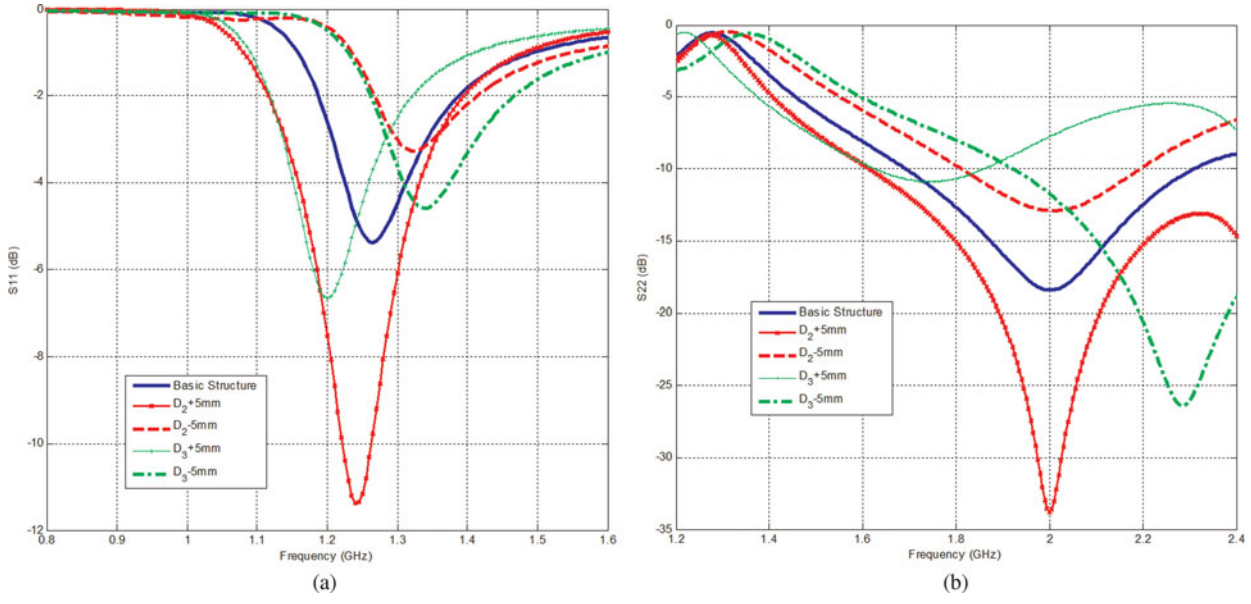

Fig. 6. Effect of D_2 and D_3 on (a) f_1 for antenna 1 (b) f_2 for antenna 2.

https://doi.org/10.1017/S1759078709990560 Published online by Cambridge University Press

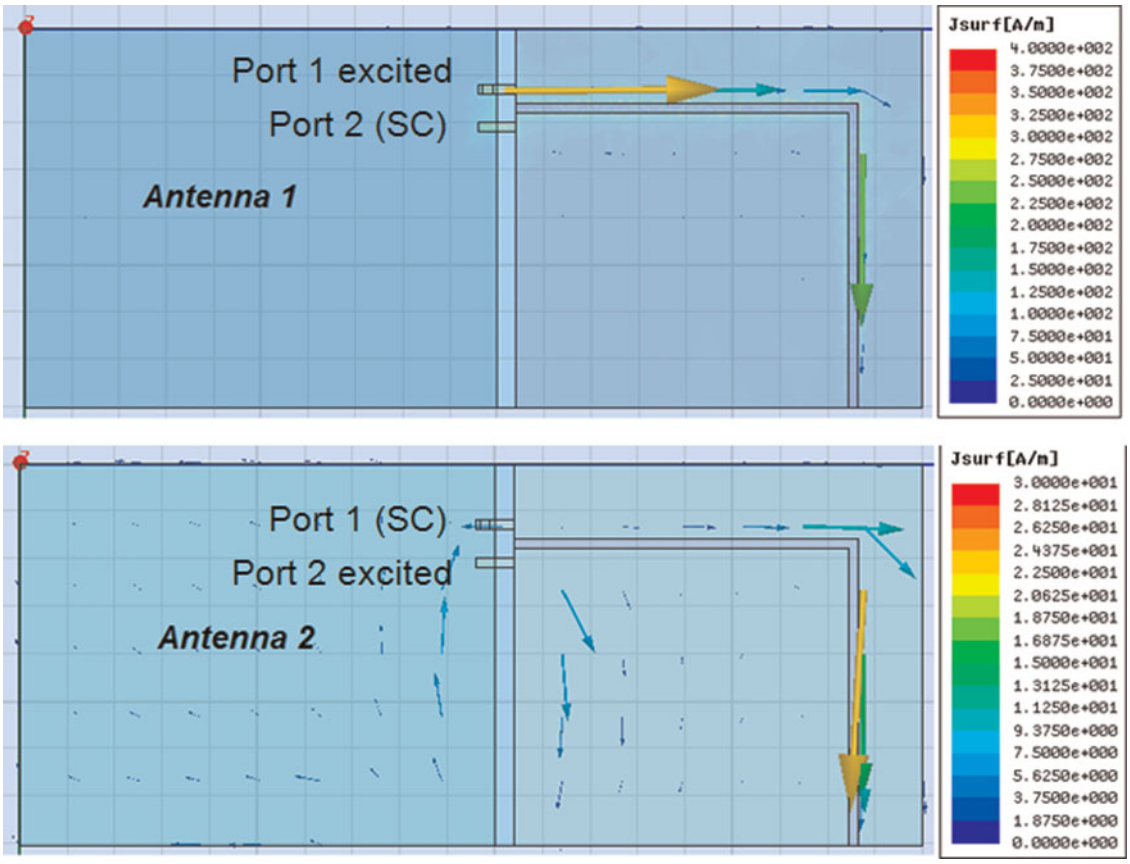

Fig. 7. Current density distribution.

An open-circuited (OC) termination is considered for the stub 2 – ($\lambda g/2$ long at f_2) connected on port 2, guarantying its transparency at frequency f_2 (OC at f_2) while providing the expected isolation at f_1 (SC at f_1), simultaneously. Fig. 8 summarizes this principle.

In addition to their fundamental role in inter-frequency band isolation, the two stubs, in association with the capacitance *C*, constitute a matching circuit over the whole operating bandwidths for both ports. The SC stub (dimensions: 1×40.7 mm^2) has a characteristic impedance $Z_{c1} = 55\ \Omega$, whereas the OC stub 2 (dimensions: 4×40.7 mm^2) has a characteristic impedance $Z_{c2} = 20\ \Omega$. This lower impedance value contributes to improve the f_2-frequency band matching conditions, while enhancing the isolation level between ports 1 and 2.

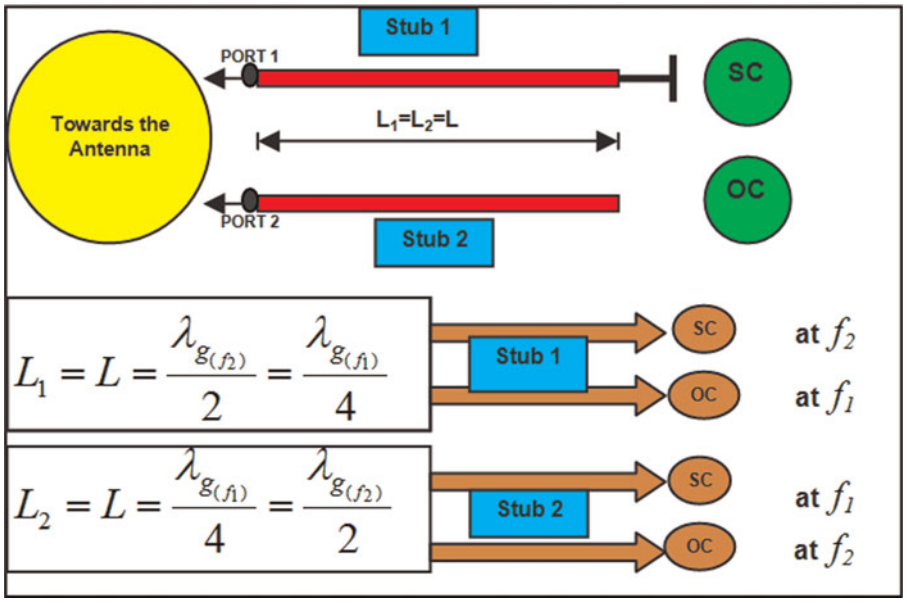

Fig. 8. Operating principle of stubs 1 and 2.

https://doi.org/10.1017/S1759078709990560 Published online by Cambridge University Press

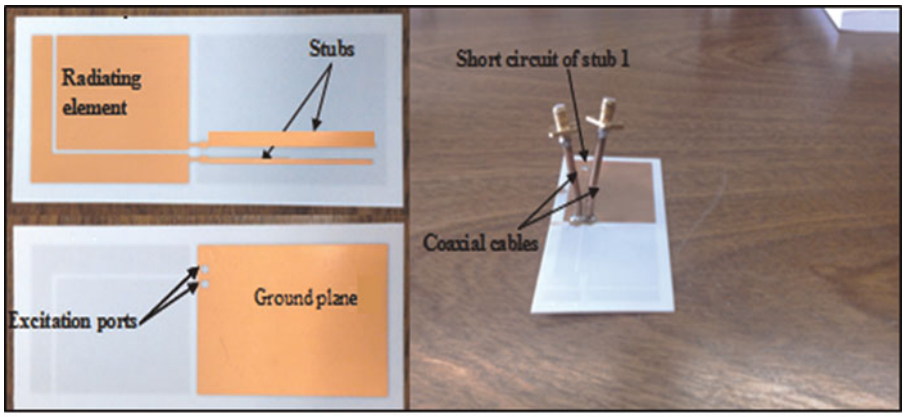

Fig. 9. Prototype of the antenna (a) without excitation (b) with excitation.

III. PROTOTYPING AND MEASUREMENTS

A) Prototype

The antenna has been optimized and processed on a $\varepsilon_r = 3.38$ Rogers^{TM} substrate (thickness $h = 0.508$ mm/tg $\delta = 0.0027$). The prototype is presented in Fig. 9(a) (before mounting the 1 pF SMD capacitance and reporting the SMA^{TM} coaxial connectors). Fig. 9(b) shows the feeding technique experimentally considered for properly exciting the antenna access ports: the central core of each coaxial cable is connected to the appropriate access ports 1 and 2 of the metallic radiating element, while their metal shielding are grounded.

B) Measurement's results and analysis

After assembling, we proceed to the S parameters measurements using a Vectorial Network Analyzer (*VNA HP_8753ES, 30 kHz–6 GHz*). The results are compared with those of the simulation in Fig. 10. Table 1 shows S parameters magnitudes at f_1 and f_2 for both simulation and measurement. The slight discrepancy is due to some approximation in the modeling of the lumped elements and cables and the PCB's solder mask; cables cause an extension of the ground plane changing slightly the input impedance, thus changing the values of return loss parameters (S_{11} and S_{22}), and increasing slightly the coupling between the two ports, thus increasing the value of S_{12}.

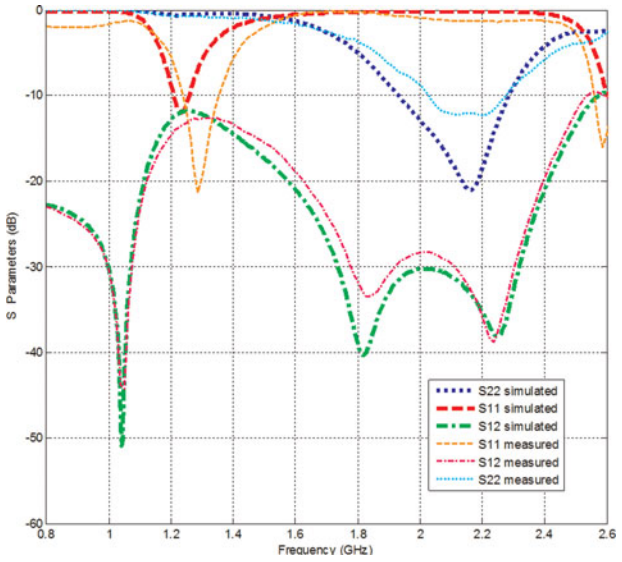

Fig. 10. Comparison between measurement and simulation.

IV. GENERALIZATION OF THE DESIGN METHOD FOR A RADIO-OPPORTUNISTIC APPROACH

A) Realization methodology

In the context of multiport antennas, the challenge lies in the isolation of adjacent access ports at different frequency bands (as well as within the same frequency band for multiports spatial sensing for instance). A relevant method is to realize a generic antenna with as many different ports as required for exciting appropriate expected operating modes and frequencies (method of characteristic modes of an antenna [8, 9]). Then, we add isolation and matching network independently from the radiating element that supports various excitation ports. Thus, the antenna can be assumed to be a lossy multipole structure, in which circuit performances (inter-bands inter-ports isolations and multiport return loss) can be optimized through this additional passive feeding network using the ADS^{TM} software (Advanced Design System from Agilent^{TM}).

Table 1. Simulation and measurement.

	Simulation	Measurement
S_{11} at f_1	−12.2 dB at 1.235 GHz	−21.4 dB at 1.288 GHz
S_{22} at f_2	−21.06 dB at 2.16 GHz	−12.31 dB at 2.2 GHz
S_{12} at f_1	−12 dB at 1.235 GHz	−12.74 dB at 1.288 GHz
S_{12} at f_2	−33.07 dB at 2.16 GHz	−35.81 dB at 2.2 GHz

https://doi.org/10.1017/S1759078709990560 Published online by Cambridge University Press

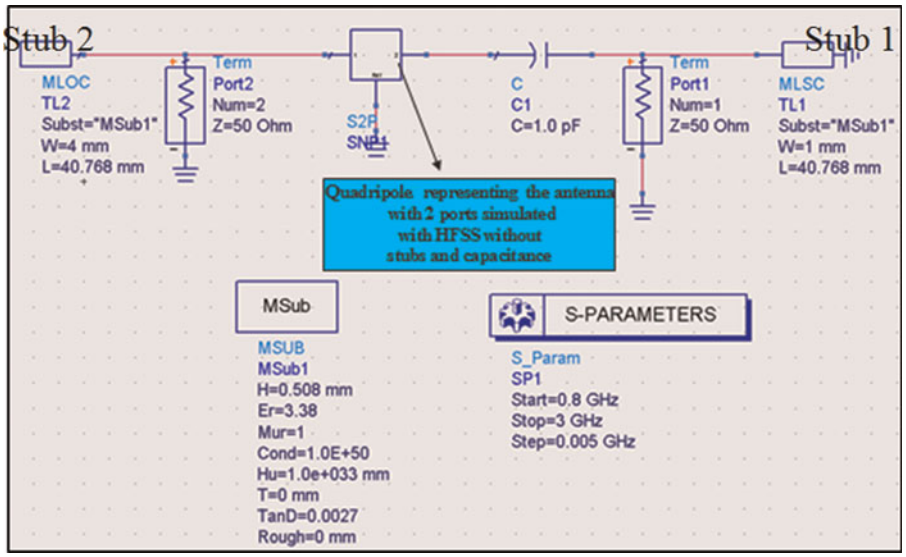

Fig. 11. Circuit simulation of the antenna.

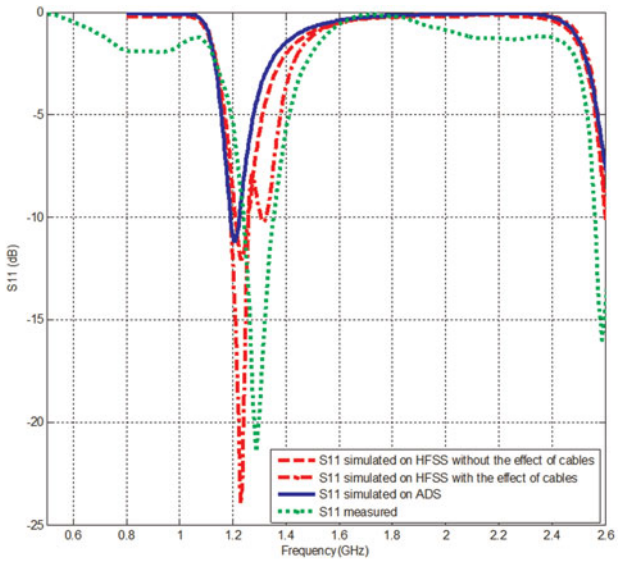

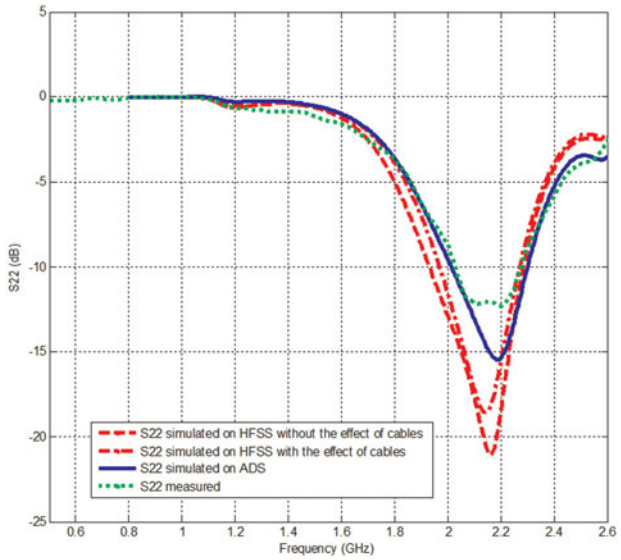

Fig. 12. Comparison of ADS, HFSS, and measurement.

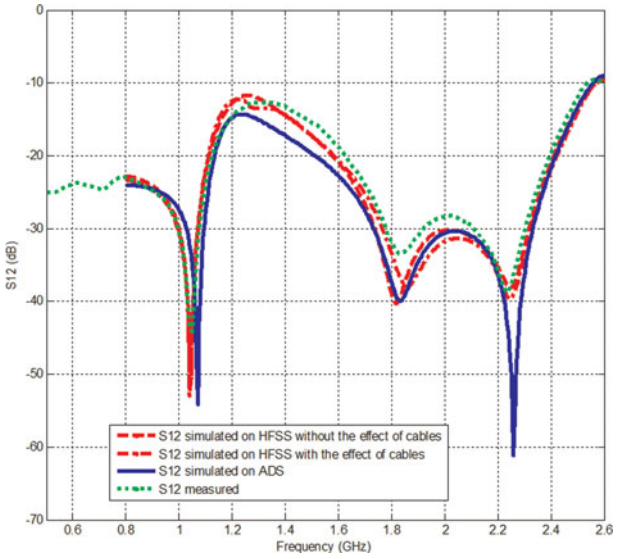

Fig. 12. (Continued)

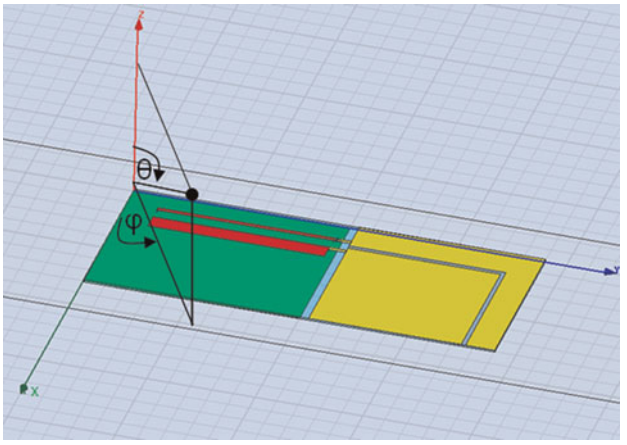

Fig. 13. Angle's convention.

https://doi.org/10.1017/S1759078709990560 Published online by Cambridge University Press

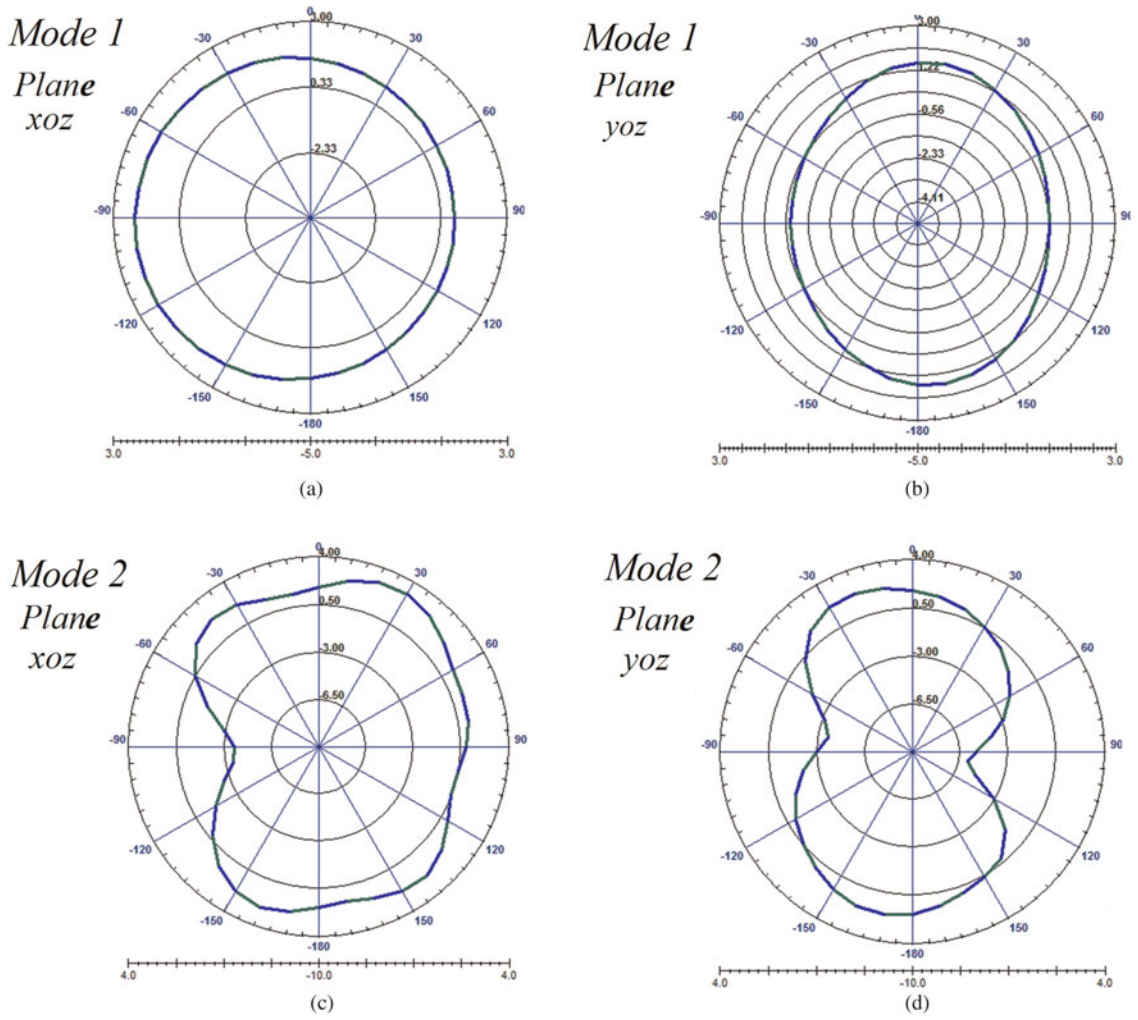

Fig. 14. Radiation patterns.

B) Optimization method

This section applies the methodology presented in Section IV.A on the above-mentioned antenna structure. A simulation of the radiating element alone (without the capacitance and stubs) is performed on an EM-simulator (HFSS from Ansoft^{TM}) to recover the [*S*] parameters of the quadripole antenna (two access ports). Then, the capacitance and the matching structures (stubs and capacitance) are added to this quadripole on ADS (Fig. 11).

We compare in Fig. 12 the results provided considering both hybrid (HFSS + ADS) and global (HFSS) electromagnetic simulations. We also consider the effect of the coaxial excitation cables connected to ports 1 and 2.

The curves show the correspondence between the EM simulations, circuit simulations, and measurements of all *S* parameters. This validates the design and optimization methodology. The discrepancy on ADS is due to the fact that the EM coupling is not taken into account with the circuit simulation.

V. RADIATION PATTERNS

We present in Fig. 13, the convention of angles and in Fig. 14, the radiation patterns in terms of directivity in the (*xoz*, $\varphi =$ 0°) and (*yoz*, $\varphi = 90°$) reference planes at f_1 (port 1: excited, port 2:50 Ω) and at f_2 (port 2: excited, port 1: 50 Ω) operating frequencies. The quasi-omnidirectional shape of the diagram in both (*xoz*) and (*yoz*) planes for both operating modes makes this antenna suitable for an opportunistic radio mobile communication. The directivity is about +2 dBi for both modes, with a *measured* maximum gain around 0 dBi, thus leading to an average 60% antenna efficiency. We note that the maximum gain is stable on the frequency band for each mode of operation because the antenna efficiency and the directivity are almost constant over these bands. A linear polarization is observed for the two modes, perpendicular to the (*xoz*) plane.

VI. CONCLUSION

A new antenna structure with two accesses simultaneously matched and isolated on two different functional frequencies is presented. It offers new prospects in the reconfigurability of antennas once digitally controlled after direct A/D conversion, and leads toward a compromise between cost/performance criteria for an RF chain operating over a wide frequency range. This structure has been produced and tested in order

https://doi.org/10.1017/S1759078709990560 Published online by Cambridge University Press

to compare measurements and simulations. An application of this antenna could be the simultaneous transmission/reception of the two Wi-Fi standards, IEEE 802.11 g ($f_1 =$ 2.4 GHz) and IEEE 802.11a ($f_2 = 5$ GHz $\approx 2f_1$).

An *n*-access antenna is being considered now. The method of characteristic modes will be considered for identifying the location of accesses before implementing feeding multiport network for controlling isolation and matching performances. Thus, a multistandard and multi-access antenna will be implemented and configured for a radio communication system based on opportunistic cognitive radio.

ACKNOWLEDGEMENTS

This work is part of the TERROP project (Opportunistic Radio Terminals) under the financial support of the National Research Agency (ANR) and the Inter-Carnot collaborative program in collaboration with the Fraunhofer Institute in Germany.

REFERENCES

[1] Harada, H.: A software defined cognitive radio prototype, in PIMRC '07, 18th Annual IEEE Int. Symp. on Personal, Indoor and Mobile Radio Communications, September 2007.

[2] Liu, Z.D.; Hall, P.S.: Dual-band antenna for hand held portable telephones. Electron. Lett., **32** (1996), 609–610.

[3] Liu, Z.D.; Hall, P.S.; Wake, D.: Dual-frequency planar inverted-F antenna. IEEE Trans. Antennas Propag., **45** (10) (1997), 1451–1458.

[4] Maci, S.; Bifi Gentili, G.; Avitabile, G.: Single-layer dual frequency patch antenna. Electron. Lett., **29** (16) (1993).

[5] Tang, I, et al.: Miniaturized hexaband meandered Pifa antenna using three meandered-shaped slits. Microw. Opt. Technol. Lett., **50** (4) (2008), 1022–1025.

[6] Mak, A.C.K., et al.: Reconfigurable multiband antenna designs for wireless communication devices. IEEE Trans. Antennas Propag., **55** (7) (2007), 1919–1928.

[7] Minard, P.; Chambelin, P.; Louzir, A.: Cost/performance optimized IEEE802.11A/B/G front end with integrated antenna diversity, in Proc. 'EuCAP 2006', Nice, France, 6–10 November 2006 (ESA SP-626, October 2006).

[8] Cabedo-Fabres, M. et al.: The theory of characteristic modes revisited: a contribution to the design of antennas for modern applications. IEEE Antennas Propag. Mag., **49** (5) (2007), 52–68.

[9] Harrington, R.F.; Mautz, J.R.: Theory of characteristic modes for conducting bodies. IEEE Trans. Antennas Propag., **AP-19** (5) (1971), 622–628.

Walid El Hajj was born in Baassir – Barja, Lebanon, on April 25, 1985. He received his degree in Electric & Electronic Engineering (Telecommunication & Computer speciality) from the Lebanese University, Faculty of Engineering, Beirut-Lebanon, in 2008. He received a National Degree of Master for research in "Microwave materials and devices for communication systems" from TELECOM BRETAGNE, Brest – France, in 2008. Since 2009, he is a Ph.D. student in Lab-STICC/MOM laboratory in the Microwave Departement in TELECOM BRETAGNE.

François Gallée received a Ph.D. degree in electronics from the University of Brest, Brest, France, in 2001. From 2001 to 2007, he was a research engineer in ANTENNESSA. His main research interest included antenna design. Currently, he is an Associate Professor within the Microwave Department, TELECOM BRETAGNE/TELECOM INSTITUT. He currently conducts research with the LABSTICC "Laboratoire en sciences et technologies de l'-information, de la communication et de la connaissance", associated with the National Research Scientific Council. His research concerns the development of new technologies for microwave and millimetre-wave applications and systems.

Christian Person received the Ph.D. degree in electronics from the University of Brest, Brest, France, in 1994.
Since 1991, he has been an Assistant Professor with the Microwave Department, Ecole Nationale Supérieure des Télécommunications de Bretagne, Brest, France. In 2003, he became a Professor with the Telecom Institute/ Telecom Bretagne, Brest, France, where he currently conducts research with the Information and Communication Science and Technology Laboratory (Lab-STICC). He is involved in the development of new technologies for microwave and millimeter-wave applications and systems. His activities are especially focused on the design of passive functions (filters, couplers) and antennas, providing original solutions in terms of synthesis techniques, analysis, and optimization procedures as well as technological implementation (foam, plastic, LTCC, etc.). He is also concerned with RF-integrated front-ends on Si, and he is presently involved in different research programs dealing with SoC/SiP antennas and reconfigurable structures for smart systems.

https://doi.org/10.1017/S1759078709990560 Published online by Cambridge University Press